Controlling Particle Size and Structural Properties of Mesoporous Silica Nanoparticles Using the Taguchi Method

ARTICLE *in* THE JOURNAL OF PHYSICAL CHEMISTRY C · JUNE 2011

Impact Factor: 4.77 · DOI: 10.1021/jp201017e

6 AUTHORS, INCLUDING:

Ya-Dong Chiang
Georgia Institute of Technology
8 PUBLICATIONS **191** CITATIONS
SEE PROFILE

Yusuke Yamauchi
National Institute for Materials Science
404 PUBLICATIONS **8,512** CITATIONS
SEE PROFILE

Kevin C.-W Wu
National Taiwan University
115 PUBLICATIONS **2,069** CITATIONS
SEE PROFILE

THE JOURNAL OF PHYSICAL CHEMISTRY C

ARTICLE

pubs.acs.org/JPCC

Controlling Particle Size and Structural Properties of Mesoporous Silica Nanoparticles Using the Taguchi Method

Ya-Dong Chiang,[†] Hong-Yuan Lian,[†] Sin-Yen Leo,[†] Shy-Guey Wang,[†] Yusuke Yamauchi,[‡] and Kevin C.-W. Wu[*,†,§]

[†]Department of Chemical Engineering, National Taiwan University, No. 1, Sec. 4, Roosevelt Road, Taipei 10617, Taiwan

[‡]World Premier International (WPI) Research Center for Materials Nanoarchitectonics, National Institute for Materials Science, 1-1 Namiki, Tsukuba 305-0044, Japan

[§]Division of Medical Engineering Research, National Health Research Institutes, 35 Keyan Road, Zhunan, Miaoli County 350, Taiwan

Supporting Information

ABSTRACT: The Taguchi method, a statistical design with an L8 orthogonal array, was adopted to optimize the synthetic conditions of mesoporous silica nanoparticles (MSNs) with respect to particle size and structural properties. The amount of the silica source (i.e., tetraethoxysilane), pH value, and reaction time were selected as significant parameters affecting the size and structural properties of the synthesized MSNs. Particle sizes ranging from 17 to 247 nm were successfully controlled by the Taguchi method, and the statistical data based on experimental results indicated that the pH value of the silica/surfactant precursor solution had a greater influence (57%) on particle size than did reaction time and the TEOS amount (29% and 13%, respectively). The effects of individual parameters on particle size and structural properties, such as surface area and structural ordering, were also investigated by changing one parameter at a time. We concluded that the pH value strongly affected mesostructural ordering and particle size. Longer reaction times in basic conditions had little effect on structural ordering but caused erosion of the MSN silica framework, resulting in smaller particle sizes. The minimum amount of TEOS for ordered MSNs was 5 mL, and more TEOS slightly increased the particle size of the synthesized MSNs. The rational design and systematic investigation of synthetic conditions for MSNs with controllable particle sizes and structural properties presented in this study show great potential for MSN-based catalytic and biomedical applications.

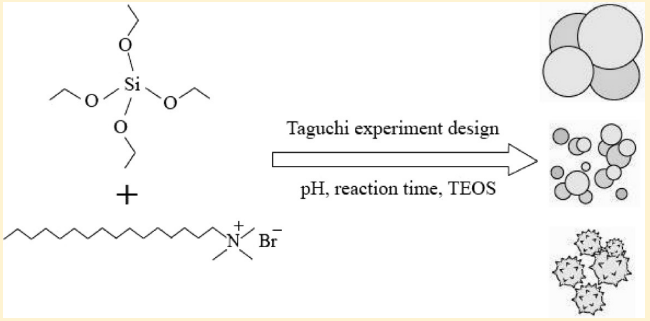

1. INTRODUCTION

Mesoporous silica materials have been intensively studied in the fields of catalysis and chromatography because of their advantages, such as high surface area, high hydrothermal stability, and diverse surface functionality.[1,2] Recently, mesoporous silica nanoparticles (MSNs) less than 1 μm in diameter have attracted a great deal of attention for biomedical applications, including cell imaging;[3] diagnosis;[4] biosensing;[5,6] and intracellular drug, gene, and protein delivery.[7−13] For these bioapplications, the control of the MSN shape and particle size is a significant issue because these parameters strongly affect the efficacy of endocytosis, sensing, and drug loading and release. For example, Lu et al. reported that MSNs with a particle size of 50 nm exhibited more cellular uptake than did MSNs with particle sizes ranging from 30 to 280 nm.[14] In comparing the cytotoxicities of mesoporous silica nanoparticles and microparticles, He et al. concluded that MSNs with small particle sizes (190−420 nm in diameter) showed significant cytotoxicity at concentrations above 25 μg/mL, whereas MSNs with a large particle size (1220 nm in diameter) showed slight cytotoxicity over a broad concentration range of 10−480 μg/mL.[15] The Lin group demonstrated the endocytosis of MSNs with spherical- and tubelike morphologies in cancerous and noncancerous cell lines, and these MSNs exhibited the unique efficiencies of endocytosis that were both morphology- and cell-line-dependent.[16]

Several researchers have reported the synthesis of MSNs with particle sizes and shapes that can be tuned by controlling synthetic parameters, such as pH, reaction time, and temperature,[17,18] and by adding functional organosilanes.[19−21] These parameters are highly associated with the hydrolysis and condensation of the silica sources (e.g., TEOS). For example, a decrease in the pH values in the reaction system (usually below 12 in a basic condition) inhibits the hydrolysis and condensation of TEOS, resulting in small particle sizes.[22] In addition, the synthetic conditions for MSNs are similar to those for silica particles made by the Stöber method,[23] the only difference being the surfactants

Received: January 31, 2011
Revised: June 6, 2011
Published: June 08, 2011

in the MSN system. Therefore, unlike the spherical morphology of the Stöber-based silica particle, any parameter affecting the phase diagram of the surfactants will also influence the morphology of the particles.[24] For example, Trewyn et al. reported the morphological control (e.g., spheres, ellipsoids, rods, and tubes) of MSNs by using room-temperature ionic liquids (RTILs) with different alkyl chain lengths.[25]

Several researchers have used additional agents or special treatments to control the particle size or morphology of MSNs. Park et al. used microwave to synthesize MSNs with sizes ranging from 200 nm to 2 μm by adding ethylene glycol.[26] The Okubo group synthesized colloidal mesoporous silica with particle sizes of 70−110 nm by the addition of ethylene glycol (EG).[27] Qiao et al. controlled particle sizes from 25 to 200 nm by adding inorganic bases and alcohols.[17] Although all of these researchers explained the mechanism of the effect of additive agents on particle size and morphology, a detailed and systematic study of the effect of the essential reaction conditions (e.g., amount of TEOS, pH value, and reaction time) on the size and morphology of the resulting MSNs has not been reported. Because there are many parameters, each with its own conditions, and the interrelationships among these parameters and conditions are extremely complex, to analyze all of the parameters and conditions would be labor-intensive and time-consuming work. Therefore, a powerful design method that can optimize the parameters and conditions with enhanced performance, yield, and productivity is necessary.

The Taguchi method is a systematic and efficient approach to designing factorial experiments.[28] The basic principle of this method is to examine the effects of experimental variables on the synthetic process using orthogonal arrays (OA) to design a minimum number of experiments.[29] In the Taguchi method, the general design of experiments (DOE) includes the study of any given system by a set of independent variables (factors) over a specific region of interest (levels).[30] Unlike conventional DOE that focuses on the average performance of a process, the DOE of the Taguchi method can be used to consider the effects of variation on the process characteristics, thus making the product or process performance insensitive to variations through the proper design of parameters.[31] This method can be used to obtain the degree of contribution of individual factors, establish the relationship between variables and operational conditions, and achieve optimum performance for a few well-defined experimental sets. This technique is popular for manufacturing processes and quality control of materials because it can save time and money in the experimental process and can provide a systematic, simple, and efficient way to optimize the process.

In this study, we use the Taguchi method to examine how certain synthetic factors, such as the amount of TEOS, pH values, or reaction time, can affect the particle size of the synthesized MSNs, as illustrated in Figure 1. Particle sizes of nanoparticles are usually measured by two methods, that is, SEM observation and dynamic light scattering (DLS). We have tried both methods for the same sample and found that the particle size measured from DLS was always larger than that from SEM observation (Supporting Information, Figure S1), which was due to the effect of solvent molecules around MSNs. In addition, there is always aggregation of MSNs in the solution, which makes at least two peaks appear in the figure of the particle size distribution. Therefore, to determine the true particle size of MSNs, we chose the method of SEM observation. We know that SEM only looks at a discrete portion (not the whole part) of the sample. To avoid

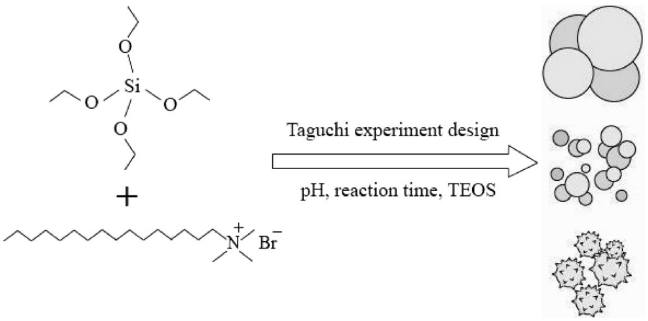

Figure 1. Schematic illustration of the control of MSN particle size by the Taguchi method.

such an erroneous judgment, we took at least five portions for one sample. In addition to particle size, we found that the surface area and pore structure of MSNs are very different due to different reaction conditions. For comparison, we also investigated the effect of each single factor on the particle size, pore structure, and morphology of MSNs.

2. EXPERIMENTAL SECTION

2.1. Synthesis of Mesoporous Silica Nanoparticles (MSNs). Conventional mesoporous silica nanoparticles were synthesized by following a published procedure,[32] but some parameters were changed according to the Taguchi design. Typically, 1 g of cetyltrimethylammonium bromide (CTAB, $C_{16}H_{33}N(CH_3)_3Br$, Aldrich) was dissolved into 480 mL of deionized water, and then NaOH (3.5 mL, 2N) was added to the CTAB aqueous solution. The pH value of the system was 12.16. The whole mixture was then heated to 80 °C before the addition of 5 mL of tetraethyl orthosilicate (TEOS, $Si(OC_2H_5)_4$, Aldrich) drop by drop at a rate of 0.5 mL min^{-1}. After the TEOS was added, the system was maintained at 80 °C for 2 h, and the white precipitate was then collected by filtration or centrifugation. To remove the residual surfactants, we washed the product with deionized water and methanol several times. Finally, the collected samples were dried in a vacuum overnight.

2.2. Selection of Factors and Levels. The hydrolysis and condensation of TEOS are two important reactions in the synthesis of silica nanoparticles. Reactions for different time periods and at different pH values affect the rates of hydrolysis and condensation of TEOS in synthetic processes. Consequently, we chose three factors, (1) amount of TEOS, (2) pH value, and (3) reaction time, to control the MSN size in this study. For each parameter, we set up three levels: (1) pH values of 9.50, 12.16, and 13.00; (2) TEOS amounts of 2.8, 5, and 15 mL; and (3) reaction times of 2, 6, and 10 h. The levels were determined based on the literature or our preliminary studies.[33] Other factors, such as reaction temperature and the adding rates of TEOS, are not considered in the present study due to their neglected effect on morphological and structural properties of MSNs, as we studied beforehand (Supporting Information, Figure S2).

Table 1 is a summary of all conditions in an L8 orthogonal array of the Taguchi experiment design. The pH value of the system was adjusted by adding NaOH (2N) or HCl (1N) before the reaction was carried out at 80 °C for 2 h. We used 1N HCl instead of 2N HCl because it was easier to control the pH values in the range of 9.50−10.00 precisely. When we prepared conventional MSNs, we found that the white precipitate appeared

Table 1. Summary of Experimental Factors and Results[a]

sample	TEOS (mL)	pH values	time (h)	particle size (nm)	surface area (m^2/g)	pore size (nm)	Structural ordering
1	2.8	9.50	2	164.9	105.74	3.01	×
2	2.8	12.16	6	210.1	1295.72	–	Δ
3	2.8	13.00	10	16.9	–	–	
4	5	9.50	6	117.6	156.57	–	×
5	5	12.16	10	171.9	894.34	2.42	○
6	5	13.00	2	109.5	969.46	2.45	○
7	15	9.50	10	31.1	236.60	–	×
8	15	12.16	2	247.1	647.55	2.66	○
9	15	13.00	6	20.9	564.91	2.55	Δ

[a] The notation of structural ordering is as follows: ○, good structural ordering; Δ, poor structural ordering; ×, no structural ordering. For sample 3, the amount of the sample was too small to be measured for nitrogen sorption analysis and XRD (marked as –). For samples 2, 4, and 7, the pore sizes of the samples could not be evaluated by the BJH method (marked as –).

after the addition of 2.8 mL of TEOS. Therefore, we chose 2.8 mL as the smallest amount of TEOS in this study. For samples that could not be collected by filtration, we used centrifugation at a high speed of 12 000 rpm for 10 min.

2.3. Characterization. The structural properties of the samples were analyzed by X-ray diffraction (XRD) on a Rigaku Ultima IV with Cu Kα radiation (40 kV, 40 mA). The morphology and structural ordering of the samples were observed with SEM (NovaTM Nano SEM) and TEM (JEOL JEM 2100F). The obtained powders were dispersed in ethanol and dropped onto copper grids for SEM and TEM observation. The porous properties of the products were analyzed using N_2 adsorption/desorption isotherms on a Micromeritics ASAP 2000 instrument. Data were evaluated using the BET and BJH methods to calculate the surface area and pore size distribution, respectively.

2.4. Analysis of Experimental Data. To analyze the results, a statistical measure of performance called the signal-to-noise (S/N) ratio is used in the Taguchi method.[34] The S/N ratios differ according to the types of characteristics and can be defined as eq 1 for the smallest number of characteristics

$$\eta = -10 \times \log\left(\frac{1}{n}\sum_{i=1}^{n} y_i^2\right) \quad (1)$$

where n is the total number of experiments in the orthogonal array and y_i is the data obtained. After the statistical analysis of the S/N ratio for each experiment, an analysis of variance (ANOVA) was employed to estimate the effectiveness of each factor.

To identify the most important factor affecting the MSN size, we calculated the variance of the target parameter. The sum of squares (S_i) of factor i at level k was calculated according to eq 2

$$S_i = \sum_{k}^{L} \frac{(\sum_{j}^{N} Y_j^2)}{N_k} - \frac{(\sum_{J}^{N}(Y_j))^2}{N} \quad (2)$$

where N is the total number of experiments, N_k is the number of levels, and Y_j is the target parameter. The total sum of squares (S_T) was calculated using eq 3:

$$S_T = \sum_{j}^{N} Y_j^2 - \frac{(\sum_{J}^{N} Y_j)^2}{N} \quad (3)$$

The experimental error was calculated using eq 4:

$$S_e = S_T - S_i \quad (4)$$

The variance of factor i (V_i) was calculated using the following equation

$$V_i = \frac{S_i}{f_i} \quad (5)$$

where f_i is the degree of freedom. The next step was the calculation of the ratio of variance (F_i), which is the quotient of the variance of factor and error according to eq 6:

$$F_i = \frac{V_i}{V_e} \quad (6)$$

The pure sum of each factor (S_i') was computed using eq 7:

$$S_i' = S_i - (f_i \times V_e) \quad (7)$$

The fraction of the effect of each factor (P_i) was calculated according to eq (8):

$$P_i = \frac{S_i'}{S_T} \times 100 \quad (8)$$

3. RESULTS AND DISCUSSION

3.1. Particle Size of MSNs Prepared by the Taguchi Method. SEM images of the samples synthesized according to the Taguchi experimental design are shown in Figure 2. The SEM images confirmed the size uniformity of the synthesized MSNs, except that of sample 2. All of the samples exhibited a spherical morphology with sizes ranging from 17 nm (sample 3) to 247 nm (sample 8). The MSN sizes in the SEM images were directly measured using photoimage process software for three experiments at three scales. The size distribution, mean particle size, and standard deviation calculated from the values are summarized in Table 1 and the Supporting Information, Table S1.

In addition to showing a spherical morphology, samples 4 and 7 exhibited urchin-like morphologies, as shown in the insets of the SEM images (Figure 2d,g). The formation mechanism of such a unique morphology is still under investigation. We suggest that the low pH values in these two samples might play a critical role because the hydrolysis and condensation rates of TEOS become very slow at low pH values (e.g., pH = 9.50). At such a low pH value, the amount of TEOS and the reaction time are very important for the control of the morphology, size, and mesostructural ordering of MSNs.[35−37] In our case, although samples 4 and 7 exhibited urchin-like morphologies, their mesostructures were not ordered, and surface areas were not high.

3.2. Statistical Analyses. The synthetic factors were analyzed by ANOVA, and size contributions from the levels of each factor are shown in Figure 3. The degree of freedom (DOF, f), sum of squares (S), mean square (variance, V), factor of variance-to-error variance ratio (F), and pure sum (S'), and the contribution percent of each factor on response (P), are summarized in

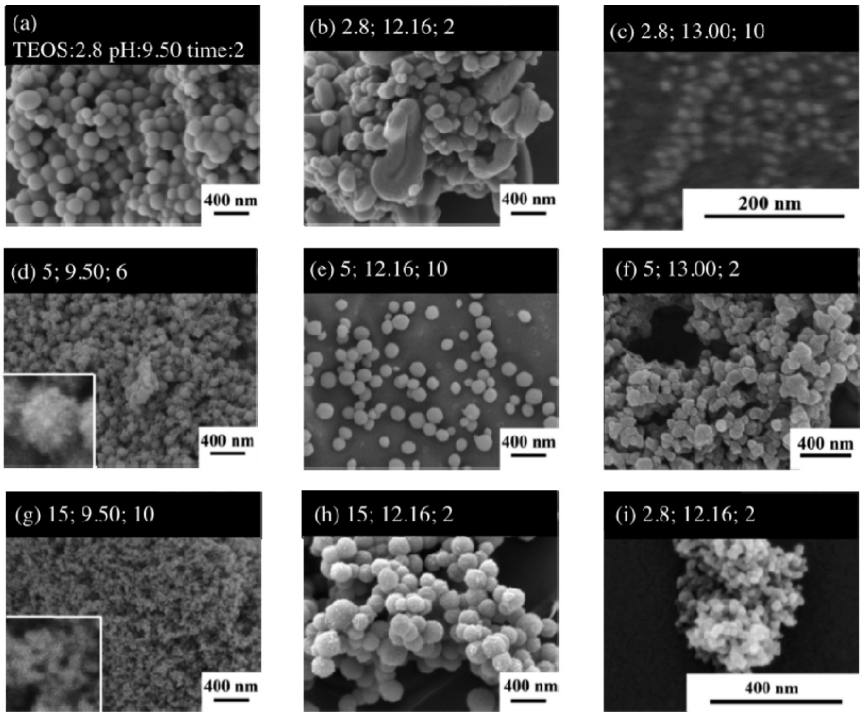

Figure 2. SEM photographs of nine samples designed by the Taguchi method. Panels a−i represent samples 1−9, respectively, in Table 1. The inset in each image indicates the amount of TEOS, pH value, and reaction time in sequence.

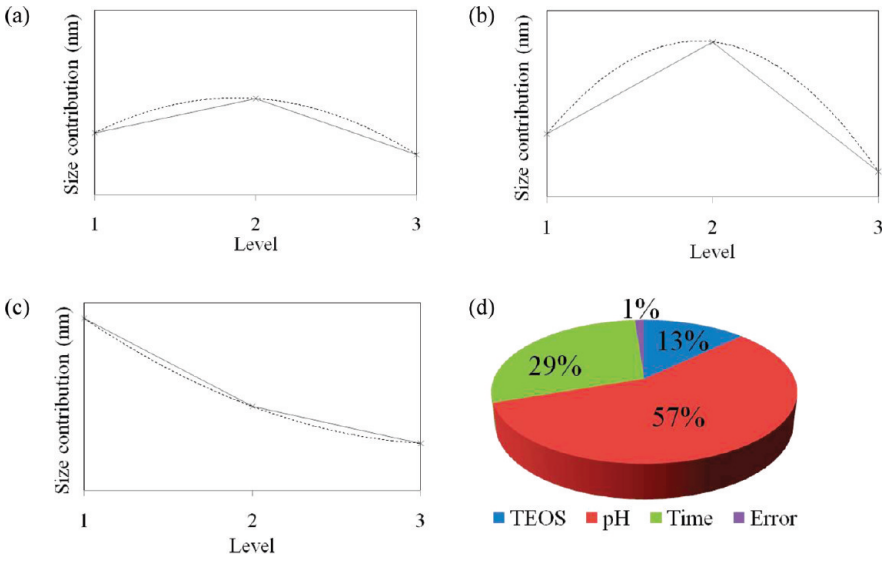

Figure 3. (a−c) Size contribution of the Taguchi method, including the effects of (a) the amount of TEOS, (b) pH value, and (c) reaction time on the particle size of synthesized MSNs. (d) The percentage of effectiveness of each factor.

Table 2. The amount of TEOS, pH value, and reaction period reached the maximum size contribution at level 2 (TEOS = 5 mL), level 2 (pH = 12.16), and level 1 (2 h), respectively. The contribution percentage of all factors for particle sizes is shown in Figure 3d. The pH value had the greatest effect (57%) on particle size, followed by reaction time (29%). Although the amount of TEOS exhibited the least influence on particle size, the percentage was still as high as 13%.

3.3. Structural Properties of MSNs Prepared by the Taguchi Method. The advantages of MSNs over solid silica nanoparticles are their ordered mesostructure, large surface area, and uniform pore size; therefore, we are also interested in the structural properties of the MSNs prepared based on the Taguchi design. The TEM images, XRD patterns, and nitrogen adsorption−desorption isotherms for samples 1−9 are shown in Figures 4 and 5. Only the samples synthesized at high pH values (12.16 or 13.00) (samples 2, 5, 6, and 8) exhibited XRD peaks, indicating that there was an ordered 2D hexagonal mesostructure in these samples (Figures 4 and 5a and Table 1). In contrast, the samples synthesized at a low pH value of 9.50

dx.doi.org/10.1021/jp201017e |J. Phys. Chem. C 2011, 115, 13158–13165

Table 2. Analysis of Variance for Particle Size Distribution

factor	DOF (f)	sum of squares (S)	variance (V)	F ratio (F)	pure sum (S')	contribution percent (P) [%]
TEOS	2	86.54	43.27	45.18	84.63	12.96
pH	2	372.49	186.25	194.46	370.57	56.75
time	2	192.04	96.02	100.26	190.13	29.12
error	2	1.91	0.96			1.17
total	8	652.99	81.62			100.00

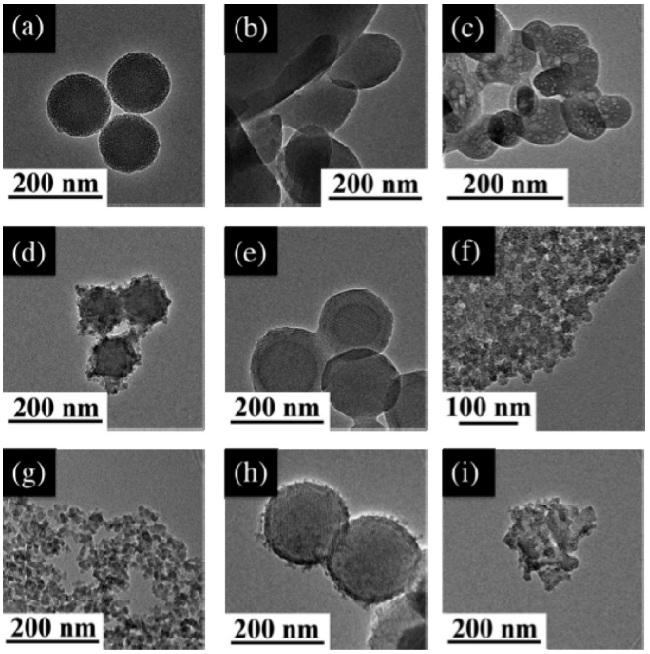

Figure 4. TEM photographs of nine samples designed by the Taguchi method. Panels a−i represent samples 1−9 in Table1, respectively.

(samples 1, 4, and 7) did not show any XRD peak, which indicated that there were no ordered mesoporous structures in these samples, as also evidenced by the TEM images. These results suggest that the pH value in the systems affects the mesostructural ordering of the synthesized materials, which is consistent with the results of previous studies.[22] In addition, samples with highly ordered mesostructures (samples 2, 5, and 6) also exhibited large surface areas (1296, 894, and 969 m^2/g, respectively). This finding is reasonable because a highly ordered structure inside the material creates a larger internal surface area. We further confirmed that MSNs with a highly ordered structure exhibited good hydrothermal stability than those with a poor or no structure, as shown in the Supporting Information, Figure S3.

The nitrogen adsorption−desorption isotherms for MSNs designed according to the Taguchi method can be classified into three groups, as shown in Figure 5b. Their corresponding pore size distributions are depicted in the Supporting Information, Figure S4. Samples 1, 4, and 7 exhibited typical Type III isotherms representing macroporous solids with multilayered adsorption.[38] The macropores likely resulted from the interspaces of small MSNs, which could also be evidenced by the hysteresis at high relative pressures. Sample 2 exhibited a Type I-like isotherm with a high surface area of around 1300 m^2/g, as shown in Figure 5b. However, a Type I isotherm would have to level off below a relative pressure of about 0.1 for the materials to be exclusively microporous. Because the isotherm for sample 2 did not level off below the relative pressure of 0.1, the sample was likely to exhibit an appreciable number of mesopores with pore sizes close to the micropore range. Other samples (5, 6, 8, and 9) exhibited Type IVc isotherms with little or no hysteresis. The adsorption in these samples proceeded via multilayer adsorption, followed by capillary condensation, resulting in an increased amount of adsorption at a higher relative pressure of around 0.2−0.4. In addition, the capillary condensation−evaporation in the mesopores was reversible, so there were few or no hysteresis loops in the isotherms.

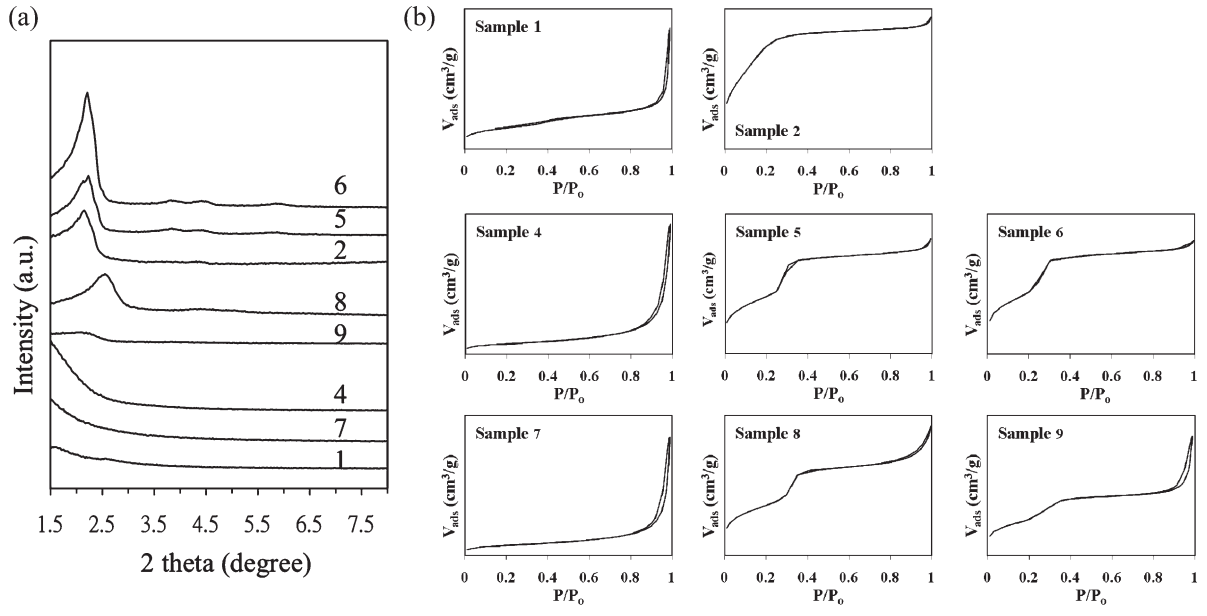

Figure 5. Characterization of the nine samples designed by the Taguchi method: (a) XRD patterns and (b) nitrogen adsorption−desorption isotherms. There was no XRD pattern or nitrogen sorption isotherm for sample 3 due to the small sample amount that could be collected by centrifugation.

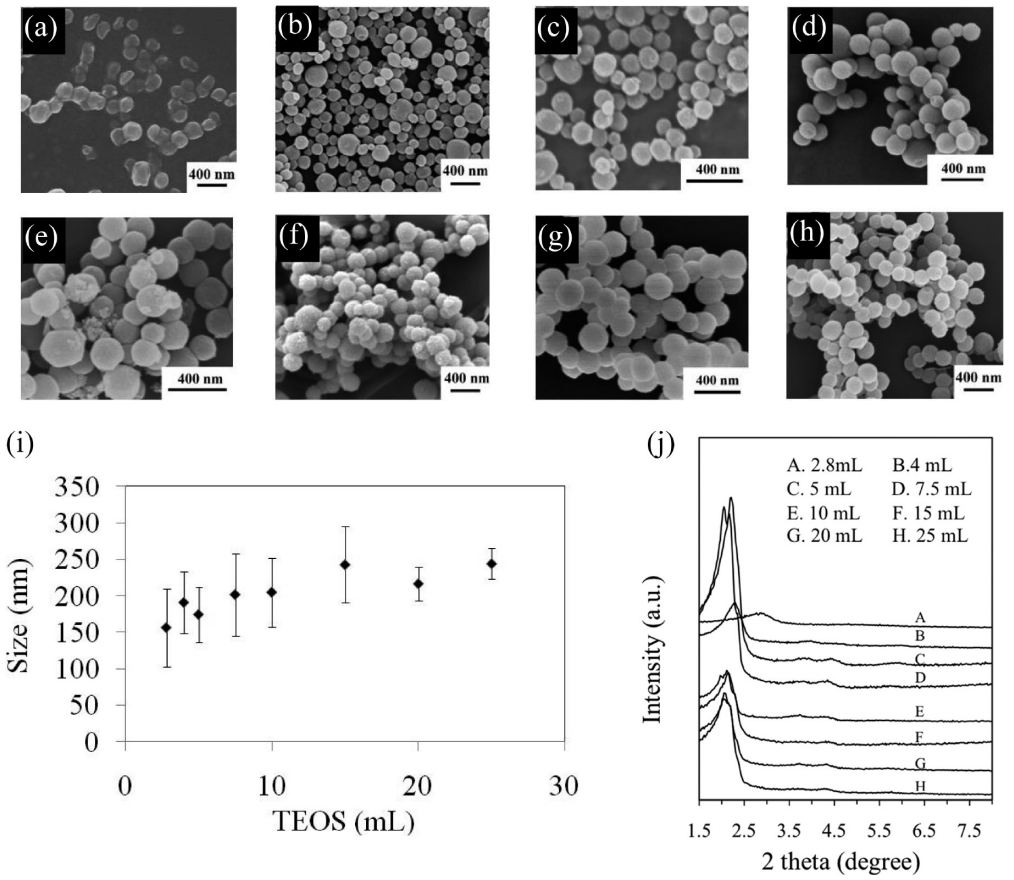

Figure 6. (a−h) SEM images of MSNs synthesized using various amounts of TEOS: (a) 2.8, (b) 4, (c) 5, (d) 7.5, (e) 10, (f) 15, (g) 20, and (h) 25 mL. (i) Relationship between particle size and amount of TEOS. (j) XRD patterns of the corresponding samples.

3.4. Effect of TEOS Amount on Particle Size and Structural Ordering. To completely investigate the effect of each factor on the particle size of MSNs, we conducted experiments in which only one factor was changed at a time. Figure 6 summarizes the effects of the amount of TEOS on the particle size and mesostructural properties of the synthesized MSNs with the reaction time maintained at 2 h and the pH at 12.16. The average particle size and standard deviation are summarized in the Supporting Information, Table S2. When the amount of TEOS was increased from 2.8 to 25 mL, the morphology of the synthesized MSN remained spherical, but the particle size was slightly increased from 160 to 240 nm, as shown in Figure 6a−h. Although an increase in the silica source (i.e., more TEOS) would be expected to result in a bigger particle size, the rate of increase of the particle size was not proportional to the increase in the amount of TEOS, as shown in Figure 6i. The data obtained here are consistent with the results of ANOVA analysis by the Taguchi method, indicating that the effect of the amount of TEOS on the particle size was small. However, we found that the amount of TEOS influenced the mesostructural ordering of the synthesized MSNs. As shown in Figure 6j, there was no peak in the XRD pattern when the amount of TEOS was 2.8 mL, which suggests that the amount of TEOS was too small to form an ordered structure. Three well-defined peaks, indexed as (10), (11), and (20), of a 2D hexagonal mesostructure were detected in two samples synthesized using 5 and 7.5 mL of TEOS. When the amount of TEOS exceeded 7.5 mL, only one broad peak appeared in the XRD pattern, indicating a wormlike or disordered mesostructure in the samples (Figure 6j, patterns D−H). Because the amount of surfactant CTAB was fixed, we can conclude that the optimal ratios for a highly ordered structure are TEOS/CTAB = 5−7.5 mL/g with a reaction time of 2 h and a pH value of 12.16.

3.5. Effects of Reaction Time on Particle Size and Structural Ordering. We studied the effects of reaction time on particle size by changing the time periods from 2, 4, and 6 to 10 h while keeping the amount of TEOS at 5 mL and the pH value at 12.16. The average particle size and standard deviation are summarized in the Supporting Information, Table S3. As shown in Figure 7a−d, the SEM images indicated that all samples exhibited a spherical morphology, and the particle sizes were all around 150−200 nm, although the size increased in the beginning and then decreased when the reaction time period increased from 2 to 10 h. When the reaction time was less than 4 h, the hydrolysis and condensation reactions of TEOS resulted in the growth of the particles. However, due to the basic condition (pH was 12.16) of the synthetic system, we supposed that the decrease in particle size resulted from the erosion of the silica framework when the reaction time was too long, as depicted in Figure 7e. Nevertheless, the competition between erosion and condensation did not affect mesostructural ordering, as evidenced in the XRD patterns (Figure 7f).

3.6. Effect of pH Value on Particle Size and Mesostructure. The pH value in the synthetic system is very important because it controls the hydrolysis and condensation rates of TEOS. We chose pH values of 9.50, 12.16, and 13.00 while keeping

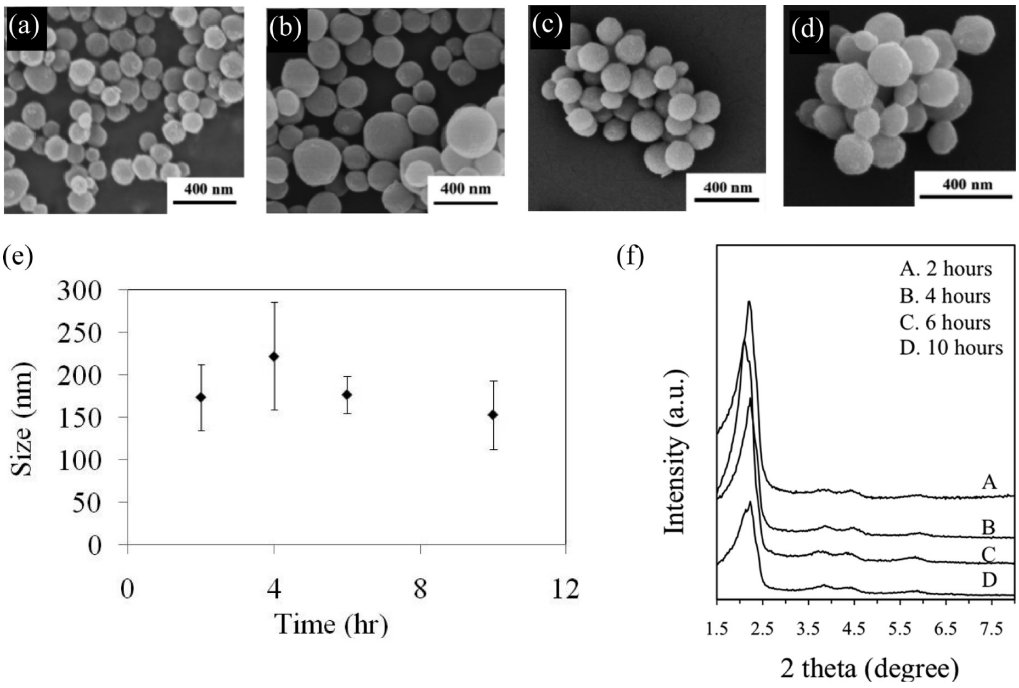

Figure 7. (a–d) SEM images of MSNs synthesized by changing reaction times: 2, 4, 6, and 10 h, respectively. (e) Relationship between particle size and reaction time. (f) XRD patterns of the corresponding samples.

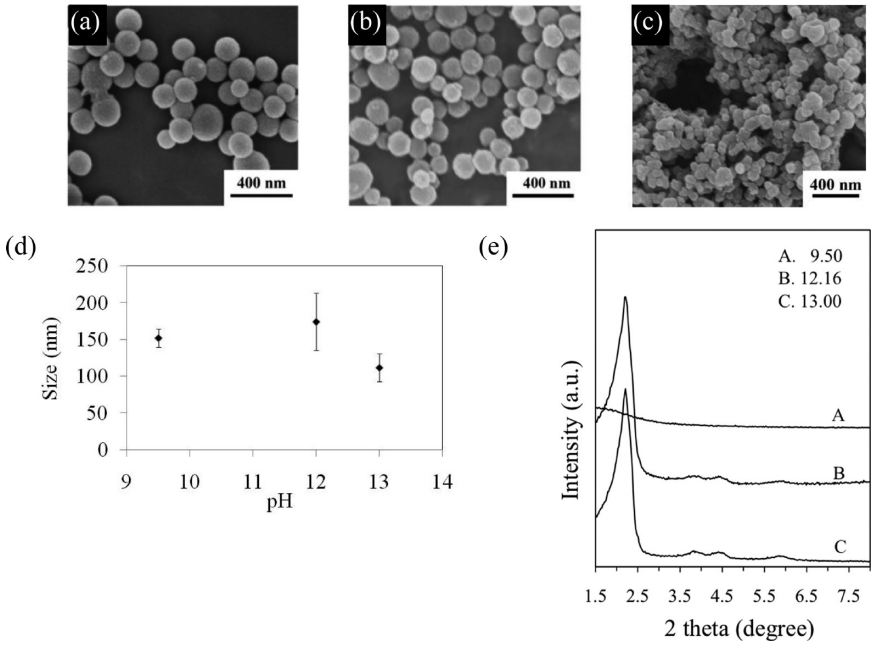

Figure 8. (a–c) SEM images of MSNs synthesized by adjusting the pH: (a) 9.50, (b) 12.16, and (c) 13.00. (d) Relationship between particle size and pH value. (e) XRD patterns of the corresponding samples.

the amounts of TEOS at 5 mL and the reaction time at 2 h to study the effect of pH on particle size and structural properties. Even so, we have found that the pH values of the three precursor solutions were going down during the reaction (Supporting Information, Figure S5). The average particle size and standard deviation are summarized in the Supporting Information, Table S4. The particle size (around 100 nm) of the sample synthesized at pH = 13.00 was smaller than the sizes of those synthesized at lower pH values (particle sizes around 150 and 180 nm for pH = 9.50 and 12.16, respectively), as shown in Figure 8a–d. This result is evidence that the silica framework of the MSNs was eroded under a basic condition (pH = 13.00). It is worth noting that there was no XRD peak for the sample synthesized at pH = 9.50 even though its spherical morphology and particle size were similar to those of samples synthesized at pH = 12.16 or 13.00, indicating that higher pH values are

essential in order to obtain a highly ordered mesostructure, as shown in Figure 8e. To comfirm that each experimental parameter affects the morphological and structural properties of MSNs independently, we changed the amount of TEOS to 15 mL while still keeping the reaction time as 2 h and studying the effect of different pH values. The results shown in the Supporting Information, Figure S6, indicated that this system (TEOS = 15 mL) exhibited the same pH effect on the morphological and porous properties of MSNs as the system of TEOS = 5 mL.

4. CONCLUSION

We have successfully controlled the particle sizes of MSNs from 17 to 247 nm based on the Taguchi design method by controlling the amount of TEOS, reaction time, and pH value. The sequence of the parameters influencing particle size was pH (57%) > reaction time (29%) > amount of TEOS (13%). In addition to particle size, the surface area of the synthesized MSNs could be controlled from around 105 to 1300 m^2/g under different conditions. The effect of individual parameters on particle size was also investigated. For example, we found that pH values strongly affected mesostructural ordering as well as particle size. Longer reaction times in basic conditions caused an erosion of the silica framework of MSNs, resulting in smaller particle sizes. The Taguchi method used in the present study provides a strategy to control both the particle size and the mesostructural properties of mesoporous silica nanoparticles, which will be useful for MSN-based biomedical and catalytic applications.

■ ASSOCIATED CONTENT

Supporting Information. Figures and tables as indicated in the text. This material is available free of charge via the Internet at http://pubs.acs.org.

■ AUTHOR INFORMATION

Corresponding Author

*E-mail: kevinwu@ntu.edu.tw.

■ ACKNOWLEDGMENT

This research was supported by the National Science Council of Taiwan (NSC 99-2119-M-002-009) and National Health Research Institutes (ME-100-PP-14).

■ REFERENCES

(1) Slowing, I. I.; Vivero-Escoto, J. L.; Trewyn, B. G.; Lin, V. S. Y. *J. Mater. Chem.* **2010**, *20*, 7924.
(2) Gallis, K. W.; Araujo, J. T.; Duff, K. J.; Moore, J. G.; Landry, C. C. *Adv. Mater.* **1999**, *11*, 1452.
(3) Lee, J. E.; Lee, N.; Kim, H.; Kim, J.; Choi, S. H.; Kim, J. H.; Kim, T.; Song, I. C.; Park, S. P.; Moon, W. K.; Hyeon, T. *J. Am. Chem. Soc.* **2010**, *132*, 552.
(4) Tian, R. J.; Zhang, H.; Ye, M. L.; Jiang, X. G.; Hu, L. H.; Li, X.; Bao, X. H.; Zou, H. F. *Angew. Chem., Int. Ed.* **2007**, *46*, 962.
(5) Slowing, I. I.; Trewyn, B. G.; Giri, S.; Lin, V. S. Y. *Adv. Funct. Mater.* **2007**, *17*, 1225.
(6) Lei, C. H.; Valenta, M. M.; Saripalli, K. P.; Ackerman, E. J. *J. Environ. Qual.* **2007**, *36*, 233.
(7) Hsiao, J. K.; Tsai, C. P.; Chung, T. H.; Hung, Y.; Yao, M.; Liu, H. M.; Mou, C. Y.; Yang, C. S.; Chen, Y. C.; Huang, D. M. *Small* **2008**, *4*, 1445.
(8) Manzano, M.; Aina, V.; Arean, C. O.; Balas, F.; Cauda, V.; Colilla, M.; Delgado, M. R.; Vallet-Regi, M. *Chem. Eng. J.* **2008**, *137*, 30.
(9) Hom, C.; Lu, J.; Tamanoi, F. *J. Mater. Chem.* **2009**, *19*, 6308.
(10) Lu, J.; Liong, M.; Li, Z.; Zink, J. I.; Tamanoi, F. *Small* **2010**, *6*, 1794.
(11) Wang, L. S.; Wu, L. C.; Lu, S. Y.; Chang, L. L.; Teng, I. T.; Yang, C. M.; Ho, J. A. A. *ACS Nano* **2010**, *4*, 4371.
(12) Rosenholm, J. M.; Sahlgren, C.; Lindén, M. *Nanoscale* **2010**, *2*, 1870.
(13) Vivero-Escoto, J. L.; Slowing, I. I.; Trewyn, B. G.; Lin, V. S.-Y. *Small* **2010**, *6*, 1952.
(14) Lu, F.; Wu, S. H.; Hung, Y.; Mou, C. Y. *Small* **2009**, *5*, 1408.
(15) He, Q. J.; Zhang, Z. W.; Gao, Y.; Shi, J. L.; Li, Y. P. *Small* **2009**, *5*, 2722.
(16) Trewyn, B. G.; Nieweg, J. A.; Zhao, Y. N.; Lin, V. S. Y. *Chem. Eng. J.* **2008**, *137*, 23.
(17) Qiao, Z. A.; Zhang, L.; Guo, M. Y.; Liu, Y. L.; Huo, Q. S. *Chem. Mater.* **2009**, *21*, 3823.
(18) Yano, K.; Fukushima, Y. *J. Mater. Chem.* **2003**, *13*, 2577.
(19) Gao, C. B.; Che, S. A. *Adv. Funct. Mater.* **2010**, *20*, 2750.
(20) Huh, S.; Wiench, J. W.; Yoo, J. C.; Pruski, M.; Lin, V. S.-Y. *Chem. Mater.* **2003**, *15*, 4247.
(21) Huh, S.; Wiench, J. W.; Trewyn, B. G.; Song, S.; Pruski, M.; Lin, V. S.-Y. *Chem. Commun.* **2003**, 2364.
(22) Schulz-Ekloff, G.; Rathousky, J.; Zukal, A. *Microporous Mesoporous Mater.* **1999**, *27*, 273.
(23) Stöber, W.; Fink, A.; Bohn, E. *J. Colloid Interface Sci.* **1968**, *26*, 62.
(24) Xing, R.; Rankin, S. E. *J. Colloid Interface Sci.* **2007**, *316*, 930.
(25) Trewyn, B. G.; Whitman, C. M.; Lin, V. S. Y. *Nano Lett.* **2004**, *4*, 2139.
(26) Park, S. E.; Kim, D. S.; Chang, J. S.; Kim, W. Y. *Catal. Today* **1998**, *44*, 301.
(27) Gu, J.; Fan, W.; Shimojima, A.; Okubo, T. *Small* **2007**, *3*, 1740.
(28) Taguchi, G. *Systems of Experimental Design*; Kraus: New York, 1987; Vol. 1, p 2.
(29) Taguchi, G. *Tables of Orthogonal Arrays and Linear Graphs*; Maruzen: Tokyo, 1962.
(30) Roy, R. K. *A Primer on the Taguchi Method*; Van Nostrand Reinhold: New York, 1990.
(31) Ross, P. J. *Taguchi Techniques for Quality Engineering*; McGraw-Hill: New York, 1988.
(32) Cai, Q.; Luo, Z. S.; Pang, W. Q.; Fan, Y. W.; Chen, X. H.; Cui, F. Z. *Chem. Mater.* **2001**, *13*, 258.
(33) Wang, S. G.; Wu, C. W.; Chen, K.; Lin, V. S.-Y. *Chem.—Asian J.* **2009**, *4*, 658.
(34) Taguchi, G. *Introduction to Quality Engineering*; Asian Productivity Organization: Tokyo, 1990.
(35) Che, S.; Sakamoto, Y.; Terasaki, O.; Tatsumi, T. *Chem. Mater.* **2001**, *13*, 2237.
(36) Schiller, R.; Weiss, C. K.; Geserick, J.; Husing, N.; Landfester, K. *Chem. Mater.* **2009**, *21*, 5088.
(37) Nakamura, T.; Mizutani, M.; Nozaki, H.; Suzuki, N.; Yano, K. *J. Phys. Chem. C* **2007**, *111*, 1093.
(38) Kruk, M.; Jaroniec, M. *Chem. Mater.* **2001**, *13*, 3169.